Intravitreal Injection of PACAP Attenuates Acute Ocular Hypertension–Induced Retinal Injury Via Anti-Apoptosis and Anti-Inflammation in Mice

Peng Lu, Yuxun Shi, Dan Ye, Xi Lu, Xiaoyu Tang, Lu Cheng, Yue Xu, and Jingjing Huang

From the State Key Laboratory of Ophthalmology, Zhongshan Ophthalmic Center, Sun Yat-sen University, Guangdong Provincial Key Laboratory of Ophthalmology and Visual Science, Guangzhou, China

Correspondence: Jingjing Huang, State Key Laboratory of Ophthalmology, Zhongshan Ophthalmic Center, Sun Yat-sen University, Guangdong Provincial Key Laboratory of Ophthalmology and Visual Science, 7 Jinsui Road, Guangzhou 510060, China; hjjing@mail.sysu.edu.cn.
Yue Xu, State Key Laboratory of Ophthalmology, Zhongshan Ophthalmic Center, Sun Yat-sen University, Guangdong Provincial Key Laboratory of Ophthalmology and Visual Science, 7 Jinsui Road, Guangzhou 510060, China; xuyue57@mail.sysu.edu.cn.

PL and YS contributed equally to this work.

Received: October 2, 2021
Accepted: February 27, 2022
Published: March 16, 2022

Citation: Lu P, Shi Y, Ye D, et al. Intravitreal injection of PACAP attenuates acute ocular hypertension–induced retinal injury via anti-apoptosis and anti-inflammation in mice. *Invest Ophthalmol Vis Sci.* 2022;63(3):18. https://doi.org/10.1167/iovs.63.3.18

Purpose. Pituitary adenylate cyclase-activating polypeptide (PACAP) has shown potent neuroprotective effects in central nervous system and retina disorders. However, whether PACAP can attenuate retinal neurodegeneration induced by acute ocular hypertension (AOH) and the underlying mechanisms remain unknown. In this study, we aimed to investigate the effects of PACAP on the survival and function of retinal ganglion cells (RGCs), apoptosis, and inflammation in a mouse model of AOH injury.

Methods. PACAP was injected into the vitreous body immediately after inducing AOH injury. Hematoxylin and eosin staining and optical coherence tomography were used to evaluate the loss of retina tissue. Pattern electroretinogram was used to evaluate the function of RGCs. TUNEL assay was used to detect apoptosis. Immunofluorescence and western blot were employed to evaluate protein expression levels.

Results. PACAP treatment significantly reduced the losses of whole retina and inner retina thicknesses, Tuj1-positive RGCs, and the amplitudes of pattern electroretinograms induced by AOH injury. Additionally, PACAP treatment remarkably reduced the number of TUNEL-positive cells and inhibited the upregulation of Bim, Bax, and cleaved caspase-3 and downregulation of Bcl-xL after AOH injury. Moreover, PACAP markedly inhibited retinal reactive gliosis and vascular inflammation, as demonstrated by the downregulation of GFAP, Iba1, CD68, and CD45 in PACAP-treated mice. Furthermore, upregulated expression of NF-κB and phosphorylated NF-κB induced by AOH injury was attenuated by PACAP treatment.

Conclusions. PACAP could prevent the loss of retinal tissue and improve the survival and function of RGCs. The neuroprotective effect of PACAP is probably associated with its potent anti-apoptotic and anti-inflammatory effects.

Keywords: PACAP, acute ocular hypertension, apoptosis, reactive gliosis, inflammation

Acute angle closure, which is more prevalent in Asian people, can lead to permanent visual impairment and irreversible blindness.[1,2] An acute attack of glaucoma is characterized by a sudden rise in intraocular pressure, usually above 70 mmHg, that results in retinal ischemia and retinal ganglion cell (RGC) loss.[3] Pressure-induced acute ocular hypertension (AOH) injury is a well-established model of acute angle closure.[4] AOH injury imitates the ischemia process in acute attacks of glaucoma and is known to result in RGC apoptosis, impairment of visual function, and inflammation.[5] Merely lowering intraocular pressure is not sufficient to treat glaucoma. Alternative neuroprotective strategies to improve the survival and function of retinal neurons are urgently needed.

Pituitary adenylate cyclase-activating polypeptide (PACAP) is an endogenous peptide with few side effects that was originally isolated from ovine hypothalamus and belongs to the vasoactive intestinal peptide, secretin, and glucagon peptide family.[6,7] PACAP and its receptors are present in the central nervous system and in retinal tissue.[7,8] PACAP was found to exert potent neuroprotective effects in animal models of neurodegenerative diseases, including Alzheimer's disease, Parkinson's disease, and cerebral ischemia injury.[9–11] A similar role for PACAP in the retina was also found in non-pressure animal models of glaucoma in several previous studies.[12–15] PACAP was found to prevent retinal tissue loss in monosodium glutamate–induced retinal injury[12] and was found to improve RGC survival through anti-apoptotic and anti-inflammatory effects in *N*-methyl-D-aspartate (NMDA)-induced retinal damage.[13,14] Our previous study also found that PACAP could inhibit RGC apoptosis induced by optic nerve crush (ONC) injury.[15] The pathogenesis and clinical characteristics of normal tension glaucoma and acute angle closure

Copyright 2022 The Authors

This work is licensed under a Creative Commons Attribution-NonCommercial-NoDerivatives 4.0 International License.

Downloaded from m.iovs.org on 05/04/2024

glaucoma are largely different.[1] Few studies have investigated the effect of PACAP in a glaucoma model of AOH injury. Seki et al.[16] found that PACAP could prevent RGC loss; however, the effect of PACAP on visual dysfunction, apoptosis, retinal reactive gliosis, and vascular inflammation induced by AOH injury, as well as the underlying mechanisms of PACAP in AOH injury, remain largely unknown.

Thus, we conducted a series of experiments to investigate the specific effects and underlying mechanisms of PACAP treatment in a mouse model of AOH injury which will aid the application of PACAP in the treatment of glaucoma.

Materials and Methods

Mouse Model of AOH Injury and PACAP Administration

Female C57BL/6J mice (6–8 week of age) were purchased from the Animal Laboratory of Zhongshan Ophthalmic Center (Guangzhou, China) and housed in temperature-controlled rooms on a 12-hour light/dark cycle. The mice were given free access to food and water. All animal care and experimental procedures were approved by the Institutional Animal Care and Use Committee of Zhongshan Ophthalmic Center (permit number SYXK 2019-175) and complied with the ARVO Statement for the Use of Animals in Ophthalmic and Vision Research.

For the induction of AOH injury, mice were anesthetized with pentobarbital. A mixture of 0.5% tropicamide and 0.5% phenylephrine eye drops was used to dilute the pupil. A 31-gauge sterile needle connected to a saline reservoir with a height of 150 cm was cannulated into the anterior chamber in the right eye. Intraocular pressure was raised to 110 mmHg for 60 minutes; the needle was then removed to allow natural retinal reperfusion.[4,17] The contralateral left eye was also cannulated while the intraocular pressure was not elevated and served as control in this study.

In the PACAP-treated group, PACAP1-38 (137061-48-4; Selleck Chemicals, Inc., Houston, TX, USA) at a concentration of 10^{-7} M was injected into the vitreous body immediately after reperfusion of the retina with a total volume of 2 µL (Fig. 1A). This concentration was selected based on our previous study.[15] A heating pad was used to prevent hypothermia in anesthetized mice, and tobramycin ointment was topically applied to prevent ocular infection. Mice were sacrificed at 1, 3, and 7 days after AOH injury (Fig. 1A) for subsequent experiments.

Selection of the Time Points of Various Experiments

The time points of histological analysis, spectral-domain optical coherence tomography (SD-OCT), Tuj1 immunofluorescence, pattern electroretinogram (PERG), terminal deoxynucleotidyl transferase dUTP nick end labeling (TUNEL), and CD45 immunofluorescence (7 days or 1 day after AOH injury) were selected based on numerous previous studies,[18–22] which found that TUNEL-positive cells and CD45-positive cells were significantly increased 1 day after AOH injury and that the retinal tissue and retinal function were significantly damaged 7 days after AOH injury. However, little is known about the time-course changes of some apoptosis-related factors (Bim, Bax, Bcl-xl, cleaved caspase-3) and inflammation-related factors (glial fibrillary acidic protein [GFAP], CD68, nuclear factor kappa B [NF-κB], and phosphorylated NF-κB [p-NF-κB]). We therefore investigated the changes of these factors at different time points with western blot. The time point that showed the most significant change was selected to investigate the effect of PACAP on the changes of these factors induced by AOH injury. In addition, the time points used for immunofluorescence of these factors (cleaved caspase-3, GFAP, and CD68) were selected based on the results of the western blot.

Histological Analysis

Histological analysis was performed 7 days after AOH injury. Paraffin-embedded sections crossing the optic disc were stained with hematoxylin and eosin (H&E) as described in our previous study.[23] The slides were then mounted with coverslips, and images were acquired with a light microscope. Two images were captured in the middle area (approximately 1100 µm away from the optic disc) on each side of the optic disc, and the thicknesses of the whole retina and sublayers of the retina, including nerve fiber layer (NFL), ganglion cell layer (GCL), inner plexiform layer (IPL), inner nuclear layer (INL), outer plexiform layer (OPL), and outer nuclear layer (ONL), were measured using ImageJ software (National Institutes of Health, Bethesda, MD, USA) and calculated as the mean of these two fields.

High-Resolution Spectral-Domain Optical Coherence Tomography

SD-OCT tests were performed 7 days after AOH injury. Mice were anesthetized and pupils were dilated as mentioned above. Horizontal and vertical high-resolution OCT images

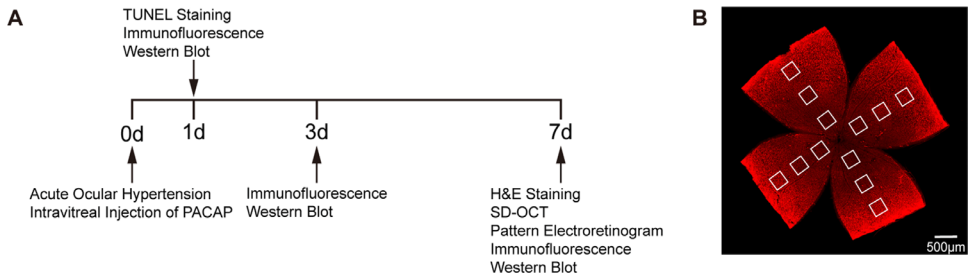

Figure 1. (A) Schematic of the timeline of inducing acute ocular hypertension injury, intravitreal injection of PACAP, and subsequent experiments. (B) Retinal flatmount image showing the 12 areas captured from the central, middle, and peripheral areas of the retina for quantification. TUNEL, terminal deoxynucleotidyl transferase dUTP nick end labeling; H&E, hematoxylin and eosin; SD-OCT, spectral-domain optical coherence tomography.

Investigative Ophthalmology & Visual Science

Downloaded from m.iovs.org on 05/04/2024

crossing the optic disc were acquired with a SD-OCT system (Envisu R4310; Bioptigen, Inc., Morrisville, NC, USA) using the radial volume scan with a diameter of 1 mm. The thicknesses of the whole retinal and ganglion cell complex (GCC, including NFL, GCL, and IPL) were measured at four sites (two sites were horizontal and another two sites were vertical) 0.42 mm away from the optic disc with Bioptigen Diver 3.4.4 software and were calculated as the mean of these four sites.

Pattern Electroretinogram

PERG was conducted 7 days after AOH injury. Mice were anesthetized and pupils were dilated as mentioned above. The mice were placed approximately 20 cm away from the stimulator monitor, with the pupils pointing laterally (approximately 45°) and upward. PERG responses were evoked using an alternating, black-and-white horizontal grating pattern displayed on a monitor with RETI-Scan 21 (Roland Consult, Brandenburg, Germany). PERG was measured with a gold wire corneal electrode. A reference electrode was inserted in the skin of the cheek, and a ground electrode was inserted in the skin near the tail. The P50–N95 amplitude was measured from the peak of the P50 wave to the trough of the N95 wave.[24,25]

Western Blot

Retina tissues were freshly dissected 1 day, 3 days, and 7 days after AOH injury and then homogenized in radioimmunoprecipitation assay buffer containing a protease and phosphatase inhibitors cocktail. Protein concentration was measured with the BCA Protein Assay Kit (BL521A; Biosharp, Hefei, China) according to the manufacturer's instructions. Protein samples (20 µg) from each sample were loaded into 15% sodium dodecyl sulfate–polyacrylamide gel electrophoresis (SDS-PAGE) gels and transferred to polyvinylidene fluoride (PVDF) membranes. The PVDF membranes were blocked with 5% nonfat powdered milk for 1 hour at room temperature (RT) and then incubated with primary antibodies (Table). Then the membranes were washed three times and incubated with corresponding horseradish peroxidase–conjugated goat anti-mouse (1:5000, A21010; Abbkine, Wuhan, China) or anti-rabbit (1:5000, A21020; Abbkine) secondary antibodies for 1 hour at RT. After washing, proteins were detected with enhanced chemiluminescence reagent (FD8030; FDbio, Hangzhou, China) using the ChemiDoc Touch Imaging System (Bio-Rad, Hercules, CA, USA). The band intensity was quantified by Image Lab 6.0 software (Bio-Rad).

Retinal Flatmount Preparation, Imaging, and Quantification

The eyeballs were enucleated 1 day or 7 days after AOH injury and were fixed in 4% paraformaldehyde for 45 minutes. The retina tissues were dissected and then permeabilized and blocked in phosphate-buffered saline containing 0.5% Triton X-100 and 5% bovine serum albumin at 4°C overnight. Subsequently, retinas tissues were incubated with primary antibodies (Table) at 4°C overnight. Then, the retinas were incubated with corresponding Alexa Fluor 488- or 555-conjugated secondary antibody (1:500, 4408S, 4412S, 4413S, 4416S; Cell Signaling Technology, Danvers, MA, USA) for 2 hours at RT. Then, 4′,6-diamidino-2-phenylindole (DAPI) was added to label the nuclei. Next, the retinas were flattened by cutting four radial incisions and mounted with microscope slides. Fluorescein images of the four quadrants of the retina (Fig. 1B) were captured with confocal laser scanning microscopy (LSM880; Carl Zeiss Meditec, Jena, Germany). For each quadrant, images were taken of the central, middle, and peripheral areas, which were approximately 500 µm, 1100 µm, and 1700 µm, respectively, away from the optic disc. A total of 12 images were obtained for each sample. The numbers of Tuj1-positive cells and CD45-positive cells in the central, middle, and peripheral areas were calculated as the mean number of the corresponding four fields. Subsequently, the total average number was calculated as the mean of all 12 fields.

Terminal Deoxynucleotidyl Transferase dUTP Nick-End Labeling

TUNEL staining was performed 1 day after AOH injury with a TUNEL kit (In Situ Cell Death Detection with Fluorescein; Roche, Munich, Germany) according to the

Table. Primary Antibody List

Antibody	Species	Company	Catalog No.	Application
Bim	Rabbit	Cell Signaling Technology	2933	Western blot
Bax	Rabbit	Cell Signaling Technology	2772	Western blot
Bcl-xL	Rabbit	Abcam	Ab32370	Western blot
Cleaved caspase-3	Rabbit	Cell Signaling Technology	9664	Western blot
GFAP	Mouse	Servicebio Technology	GB12096	Western blot
CD68	Rabbit	Cell Signaling Technology	97778	Western blot
NF-κB	Rabbit	Cell Signaling Technology	8242	Western blot
p-NF-κB	Rabbit	Cell Signaling Technology	3033	Western blot
GAPDH	Rabbit	ABclonal	A19056	Western blot
β-actin	Rabbit	Servicebio Technology	GB11001	Western blot
Tuj1	Mouse	BioLegend	801202	Immunofluorescence
CD45	Rat	BD Pharmingen	550539	Immunofluorescence
Cleaved caspase-3	Rabbit	Cell Signaling Technology	9579	Immunofluorescence
Alexa Fluor 568 isolectin GS-IB_4 conjugate	N/A	Invitrogen	121412	Immunofluorescence
Cy3-conjugated anti-GFAP	N/A	MilliporeSigma	MAB3402C3	Immunofluorescence
Iba1	Rabbit	Wako Chemicals	019-19741	Immunofluorescence
CD68	Rat	Bio-Rad Laboratories	MCA1957	Immunofluorescence

Investigative Ophthalmology & Visual Science

Downloaded from m.iovs.org on 05/04/2024

manufacturer's instructions. In brief, the frozen sections were incubated with the TUNEL kit for 2 hours at 37°C, and the nuclei were stained with DAPI. Fluorescein images were captured in the central, middle, and peripheral areas on each side of the optic disc using confocal laser scanning microscopy (LSM880; Carl Zeiss Meditec), and six images were obtained for each sample. The number of TUNEL-positive cells of the GCL, INL, and ONL was measured in the central, middle, and peripheral areas of the retina and calculated as the mean of the corresponding two fields. The total average number of TUNEL-positive cells of each layer was calculated as the mean of all six fields.

Retinal Cryosection

After enucleation, eyeballs were fixed in 4% paraformaldehyde overnight and dehydrated in 10% sucrose for 0.5 hour, 20% sucrose for 2 hours, and 30% sucrose overnight. Eyeballs were then embedded in Tissue-Tek optimal cutting temperature compound (Sakura Finetek, Torrance, CA, USA), frozen, and cut into 10-µm-thick slices. The cryosections were incubated with primary antibody (Table) and the corresponding secondary antibody as mentioned above. Fluorescein images were photographed in the central, middle, and peripheral areas on each side of the optic disc with confocal laser scanning microscopy (LSM880; Carl Zeiss Meditec), and six images were obtained for each sample. The numbers of certain positive cells in the central, middle, and peripheral areas were calculated as the mean of the corresponding two fields. The total average number of certain positive cells was calculated as the mean of all six fields.

Statistical Analysis

All experiments in this study were performed at least three times in each group. Each point shown in the statistical graphs indicates an individual data point. Statistical analyses were performed using Prism 7 (GraphPad, San Diego, CA, USA). Data are presented as means ± standard error of mean (SEM) and were analyzed using one-way analysis of variance (ANOVA) followed by Tukey's post hoc test. $P < 0.05$ was considered statistically significant.

Results

PACAP Attenuated the Loss of Retina Tissue After AOH Injury in Isolated Retinas

To investigate the effect of PACAP on histological change after AOH injury, H&E staining was performed 7 days after AOH injury in isolated retinas. H&E staining (Figs. 2A–2C) showed that the thicknesses of the whole retina and sublayers of the inner retina (the NFL/GCL, IPL and INL) were significantly reduced after AOH injury, but not the OPL and ONL. However, the loss of thickness in the whole retina and sublayers of the inner retina was significantly attenuated in PACAP-treated retinas.

PACAP Attenuated the Loss of Retina Tissue After AOH Injury in Live Mice

SD-OCT scanning performed in live mice could better reflect the real condition of post-AOH retinal tissue damage. SD-OCT results (Figs. 2D–2F) demonstrated that the thicknesses of the whole retina and the GCC were markedly decreased after AOH injury, with the change in the GCC being more significant. However, these changes were partly reversed when treated with PACAP, further confirming that PACAP treatment could reduce the loss of retina tissue after AOH injury.

PACAP Improved the Survival of RGCs after AOH Injury

Next, we assessed the effect of PACAP on the survival of RGCs after AOH injury by counting the number of Tuj1-positive cells. The results of retinal flat mounts showed that the numbers of Tuj1-positive RGCs in all areas of the retina were significantly reduced 7 days after AOH injury, and PACAP treatment retained a fair number of RGCs (Fig. 3). Our results demonstrate that PACAP could improve the survival of RGCs after AOH injury.

PACAP Attenuated the Loss of Visual Function After AOH Injury

A significant decrease in the number of RGCs that was induced by AOH injury might affect the visual function of mouse eyes. Therefore, we applied PERG to assess the effect of PACAP on the function of RGCs in AOH injury. The P50–N95 amplitude of the PERG was markedly reduced in mice 7 days after AOH injury compared with that of the control mice, whereas the amplitude was well preserved by PACAP treatment in AOH injury (Fig. 4). Our results indicate that PACAP treatment could attenuate the loss of RGC function in AOH injury.

PACAP Inhibited Apoptosis of RGCs Induced by AOH Injury

Apoptosis is a critical event involved in retinal neuronal death after AOH injury.[26] TUNEL staining was performed to preliminarily evaluate the anti-apoptotic effect of PACAP in AOH injury. TUNEL-positive cells were notably increased in the central, middle, and peripheral areas of the GCL and INL but not in the ONL 1 day after AOH injury when compared with the control (Fig. 5). In contrast, the number of TUNEL-positive cells was significantly reduced in the GCL and INL following treatment with PACAP (Fig. 5).

We further assessed the effect of PACAP on the expression levels of apoptosis-related factors including Bim, Bax, Bcl-xL, and cleaved caspase-3. Western blot analyses showed that the expressions of Bim, Bax, and cleaved caspase-3 were upregulated after AOH injury and peaked at day 3, whereas these changes were alleviated by PACAP treatment (Figs. 6A, 6B, 6D). The immunofluorescence result for cleaved caspase-3 was consistent with the western blot results and showed that PACAP treatment significantly reduced the number of cleaved caspase-3–positive cells, which were mainly located in the GCL (Figs. 6E–6I). The expression of Bcl-xL as demonstrated in western blot was downregulated after AOH, with a trough at day 7 (Fig. 6C). However, PACAP treatment significantly inhibited the downregulation of Bcl-xL after AOH injury (Fig. 6C). Collectively, these results indicate that PACAP exerted a potent anti-apoptotic effect in AOH injury, at least partly through the modulation of apoptosis-related factors.

Investigative Ophthalmology & Visual Science

Downloaded from m.iovs.org on 05/04/2024

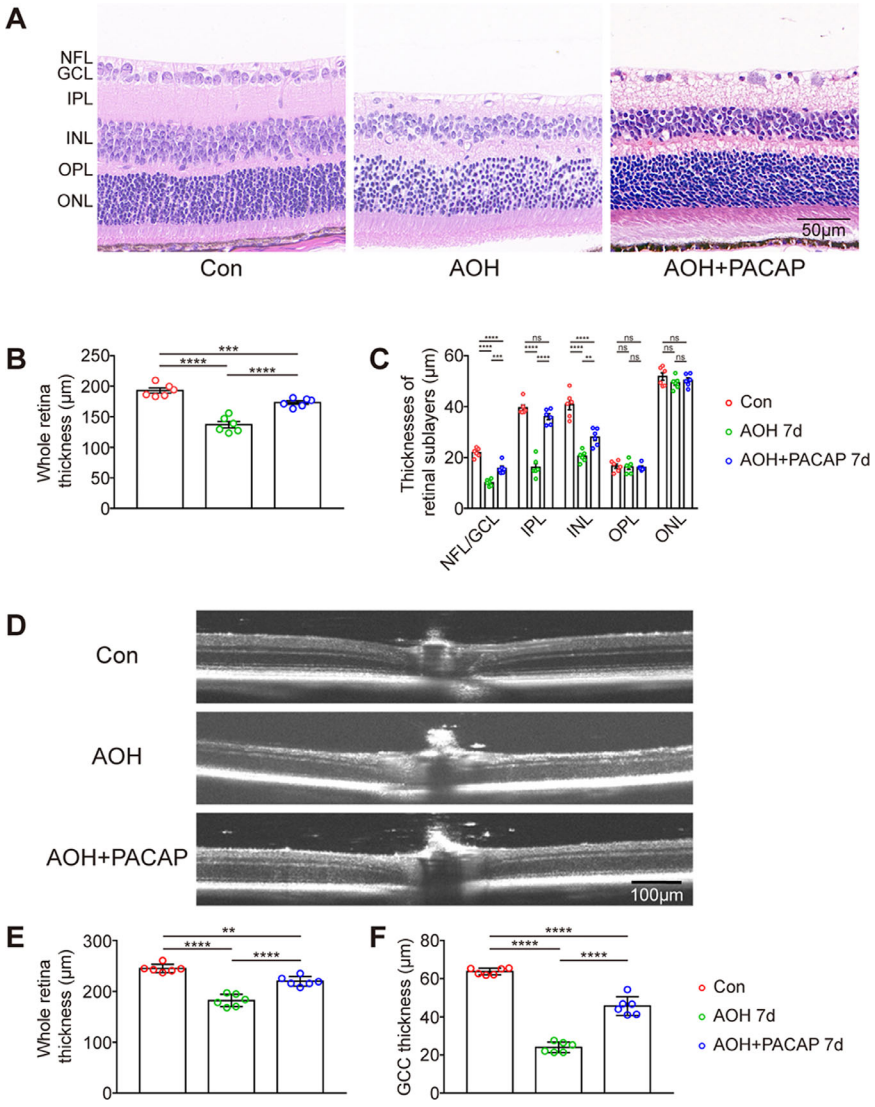

Figure 2. PACAP treatment inhibited the loss of retinal tissue. (**A**) Representative H&E staining images of retinal sections 7 days after AOH injury (magnification 40×). (**B**, **C**) Bar charts showing the quantitative analyses of whole retina thickness and retinal sublayer thicknesses of different groups in H&E staining ($n = 6$, two images per sample). (**D**) Representative SD-OCT scanning performed in live mice 7 days after AOH injury. (**E**, **F**) Bar charts showing the quantitative analyses of whole retina thickness and GCC thickness of different groups by SD-OCT examination ($n = 6$, four images per sample). Data are shown as mean ± SEM and were analyzed using ANOVA followed by Tukey's post hoc test. $^{**}P < 0.01$, $^{***}P < 0.001$, $^{****}P < 0.0001$. Each point shown in the bar charts indicates an individual data point.

PACAP Ameliorated the Reactive Gliosis After AOH Injury

Reactive gliosis was found to occur in AOH injury and to be associated with further retinal neuronal death.[27] To investigate whether PACAP treatment could alleviate the reactive gliosis induced by AOH injury, we explored the expression of GFAP, a specific marker of macroglia including astrocytes and Müller cells. As shown in the western blot results, GFAP was significantly increased after AOH injury and peaked at day 7, whereas PACAP significantly inhibited the upregulation of GFAP 7 days after AOH injury (Fig. 7A). Consistently, immunofluorescence results for GFAP showed that the expression of GFAP as quantified by percent area was also markedly upregulated in the central, middle, and peripheral areas of the retina after AOH injury (Figs. 7B–7F). Additionally, thickened cell bodies and outward extension of the processes from the NFL to the ONL of GFAP-positive cells were found after AOH injury (Fig. 7B), whereas these changes were attenuated with the PACAP treatment (Fig. 7B).

Moreover, we investigated the effect of PACAP on changes in microglia and macrophages (these two cell populations are antigenically not distinguishable and henceforth are referred to as microglia/macrophages[28,29]) in AOH injury. Western blot analysis of CD68, a specific marker of activated microglia/macrophages, showed that the expression of CD68 was upregulated soon after AOH injury, with a peak at day 3 (Fig. 8A). Fluorescence double-labeling of CD68 and Iba1 (a specific marker of all microglial/macrophage cells) was performed 3 days after AOH injury. Significant morphological changes (reduced branches, larger and rounder soma) and enhanced migration (from the IPL and

Investigative Ophthalmology & Visual Science

Downloaded from m.iovs.org on 05/04/2024

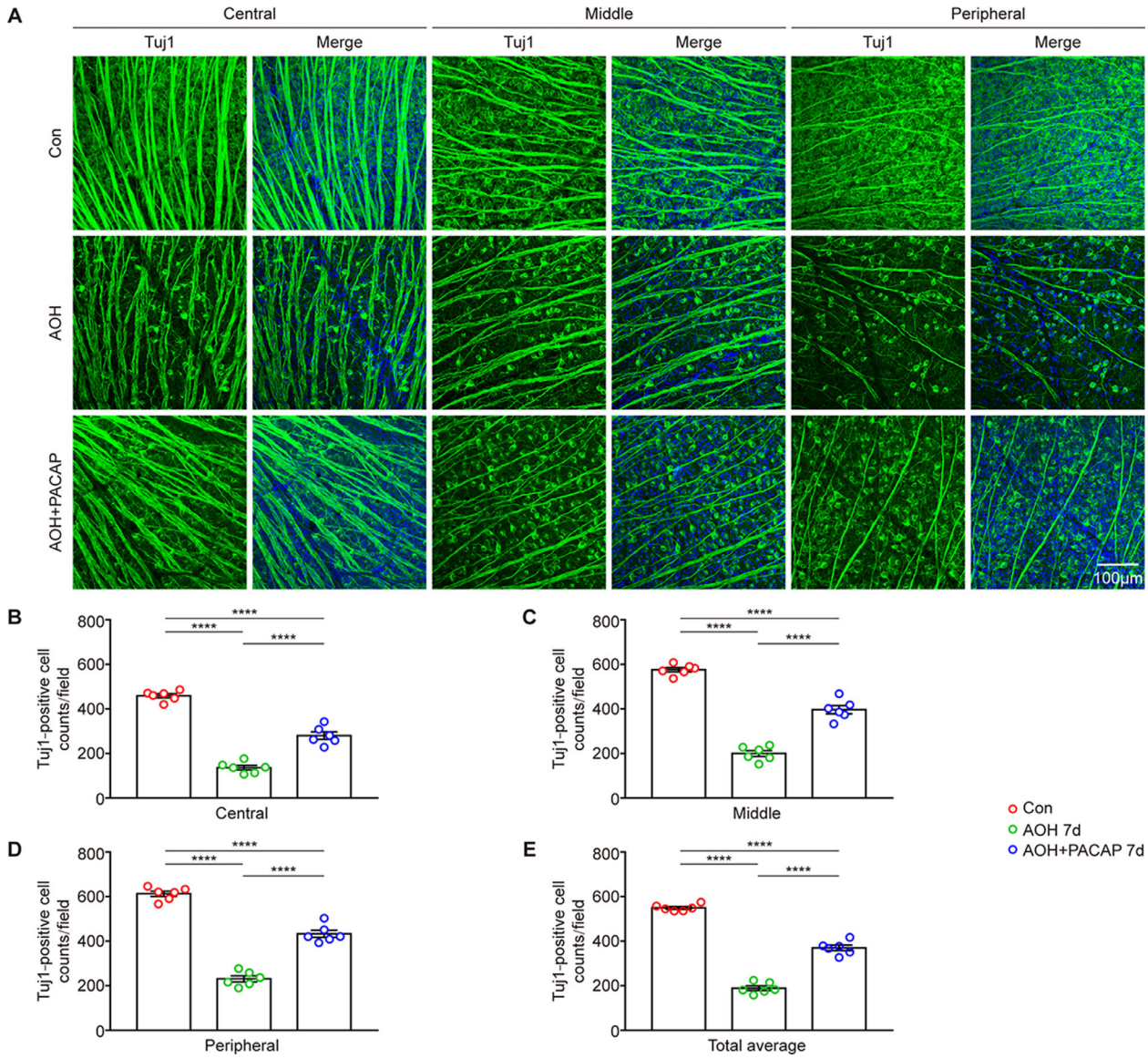

Figure 3. PACAP treatment improved the survival of RGCs after AOH injury. RGCs were labeled by Tuj1. (**A**) Representative images of retinal flatmounts labeled with Tuj1 (*green*) and DAPI (*blue*) 7 days after AOH injury (magnification 20×). (**B–E**) Bar charts showing the quantitative analyses of Tuj1-positive RGC counts in the central, middle, and peripheral areas of the retina ($n = 6$, four images per sample) and the total average number of Tuj1-positive RGCs ($n = 6$, 12 images per sample) of different groups. Data are shown as mean ± SEM and were analyzed using ANOVA followed by Tukey's post hoc test. $^{****}P < 0.0001$. Each point shown in the bar charts indicates an individual data point.

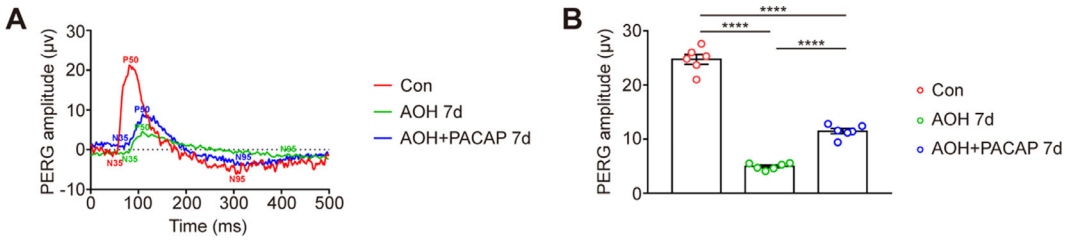

Figure 4. PACAP treatment preserved the function of RGCs, as assessed by PERG in AOH injury. (**A**) Representative PERG waveform performed 7 days after AOH injury of different groups. (**B**) Bar chart showing the quantitative analysis of PERG P50–N95 amplitudes ($n = 6$). Data are shown as mean ± SEM and were analyzed using ANOVA followed by Tukey's post hoc test. $^{****}P < 0.0001$. Each point shown in the bar chart indicates an individual data point.

Investigative Ophthalmology & Visual Science

Downloaded from m.iovs.org on 05/04/2024

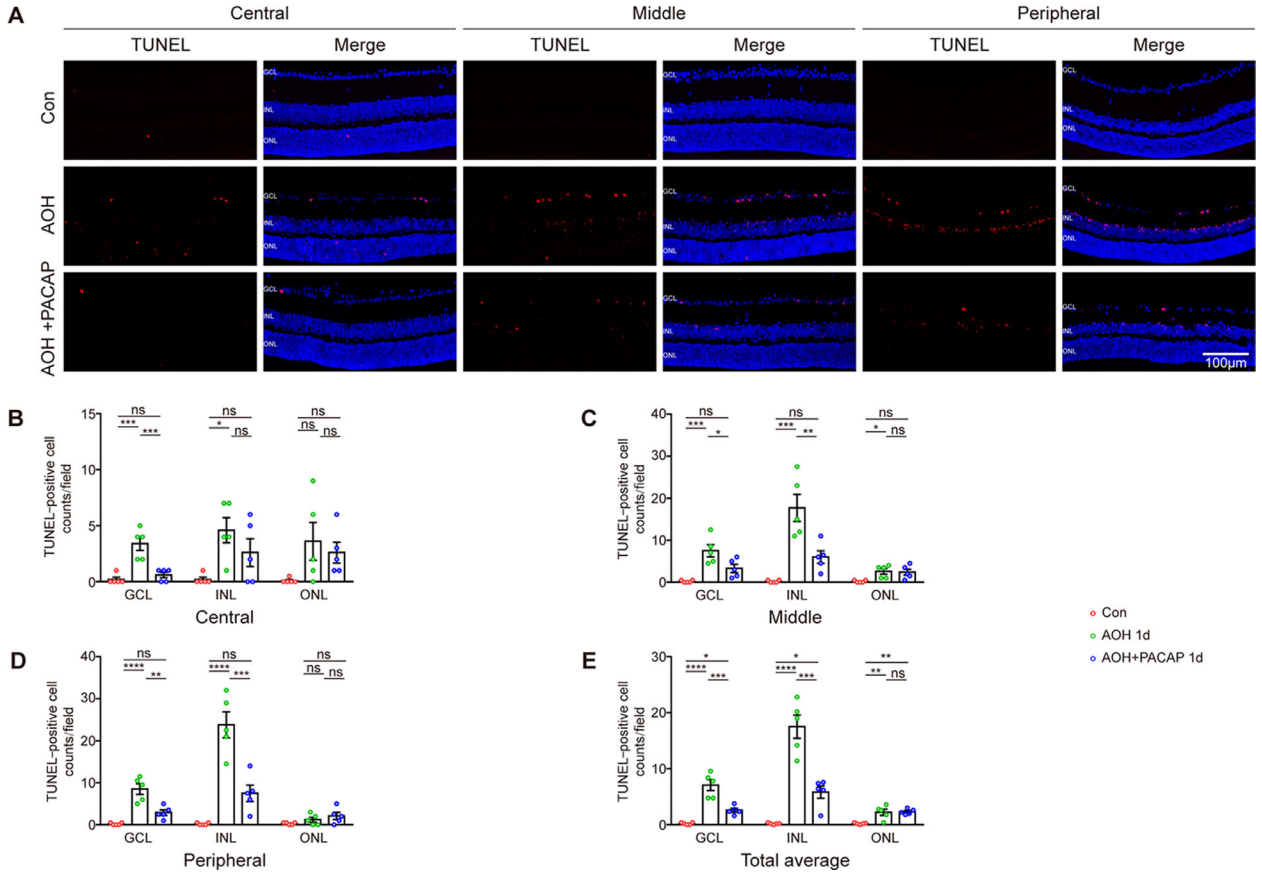

Figure 5. PACAP treatment reduced the number of TUNEL-positive cells 1 day after AOH injury. (**A**) Representative images of retinal frozen sections labeled with TUNEL (*red*) and DAPI (*blue*) 1 day after AOH injury (magnification 20×). (**B**–**E**) Bar charts showing the quantitative analyses of TUNEL-positive cell counts in the central, middle, and peripheral areas of the retina ($n = 5$, two images per sample), and the total average number of TUNEL-positive cells ($n = 5$, six images per sample) of different groups. Data are shown as mean ± SEM and were analyzed using ANOVA followed by Tukey's post hoc test. $^{*}P < 0.05$, $^{**}P < 0.01$, $^{***}P < 0.001$, $^{****}P < 0.0001$. Each point shown in the bar charts indicates an individual data point.

OPL to the GCL and INL) were found in Iba1-positive cells after AOH injury (Fig. 8B). In addition, the number of Iba1/CD68-positive cells was significantly increased after AOH injury (Figs. 8B–8F). These results indicate that microglial/macrophage cells were overactivated after AOH injury. When treated with PACAP, Iba1-positive cells showed a more ramified shape and reduced migration (Fig. 8B). Moreover, the number of Iba1/CD68-positive cells was also notably reduced (Figs. 8B–8F). Together, these results indicate that PACAP treatment effectively attenuated the overactivation of macroglia and microglia/macrophages after AOH injury.

PACAP Inhibited the Retinal Vascular Inflammation Induced by AOH Injury

AOH injury was reported to induce retinal vascular inflammation, which is characterized by leukocyte attachment to retinal blood vessels and infiltration into retina and is associated with further neuronal injury.[18] We therefore labeled all leukocytes with CD45 and labeled vessels with IB_4 to investigate the effect of PACAP on the retinal vascular inflammation in AOH injury. As shown in Figure 9, the number of CD45-positive leukocytes, which colocalized mainly with the intermediate-sized peripheral blood vessels and infiltrated into the retina, was significantly increased in the central, middle, and peripheral areas 1 day after AOH injury, whereas such increases were significantly redressed by PACAP treatment. The results demonstrated that retinal vascular inflammation induced by AOH injury could be effectively inhibited by PACAP treatment.

PACAP Inhibited Activation of the NF-κB Pathway After AOH Injury

Previous studies have shown that activation of NF-κB was involved in AOH injury and subsequent RGC death.[30,31] We therefore investigated whether PACAP treatment could inhibit activation of the NF-κB pathway in AOH injury. P-NF-κB is the activated form of NF-κB; western blot analyses showed that both NF-κB and p-NF-κB were significantly increased after AOH injury, whereas PACAP treatment significantly inhibited upregulation of NF-κB and p-NF-κB 3 days after AOH injury (Fig. 10). These results indicate that PACAP treatment could inhibit the upregulation of total and phosphorylated NF-κB after AOH injury.

Investigative Ophthalmology & Visual Science

Downloaded from m.iovs.org on 05/04/2024

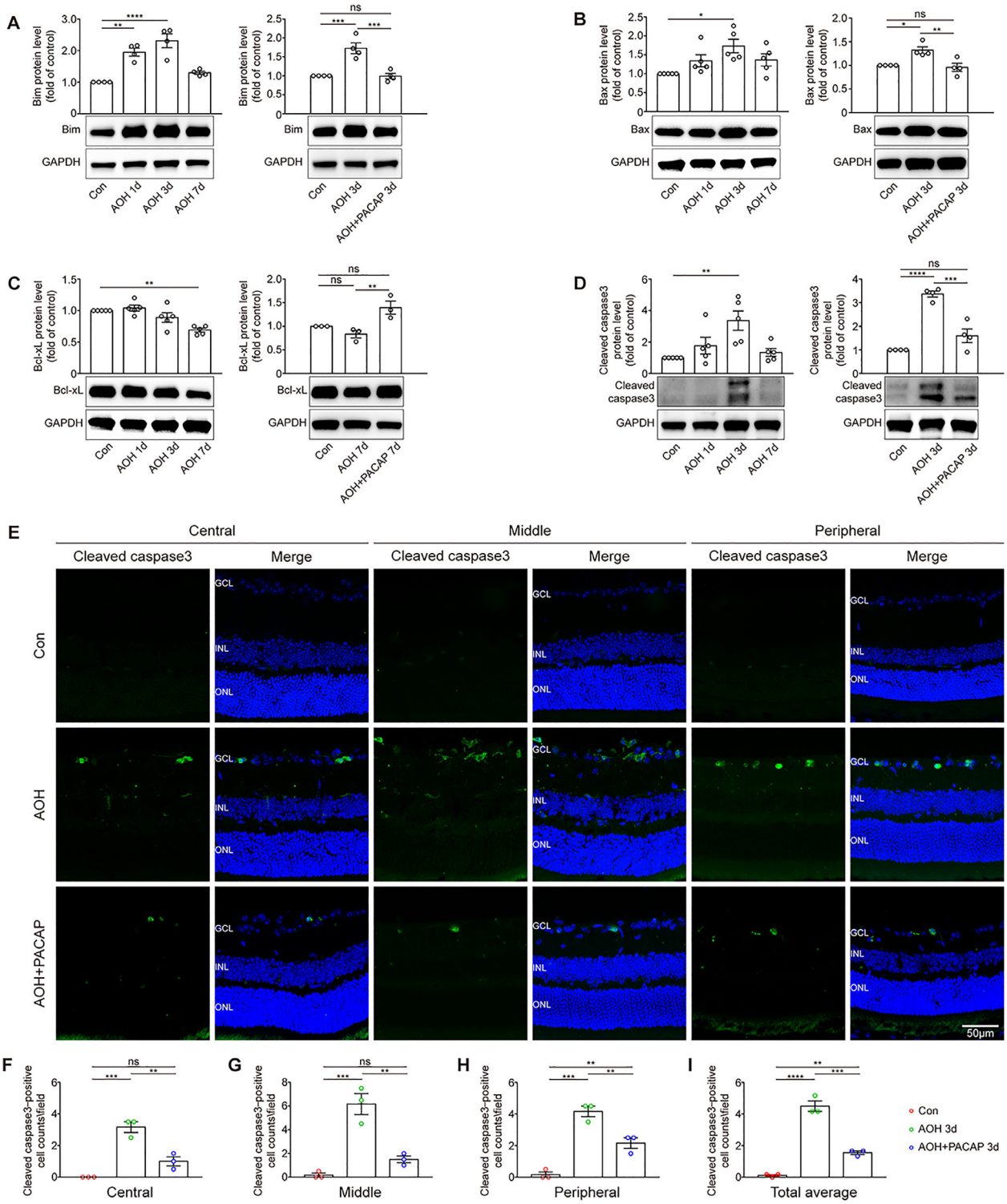

Figure 6. The effect of PACAP on the expression levels of apoptosis-associated factors. (**A–D**) The expression of Bim, Bax, Bcl-xL, and cleaved caspase-3 was evaluated by western blot ($n = 3$–5). Glyceraldehyde 3-phosphate dehydrogenase (GAPDH) was used to ensure equal loading. (**E**) Representative images of retinal frozen sections labeled with cleaved caspase-3 (*green*) and DAPI (*blue*) 3 days after AOH injury (magnification 40×). (**F–I**) Bar charts showing the quantitative analyses of average cleaved caspase-3–positive cell counts in the central, middle, and peripheral areas of the retina ($n = 3$, two images per sample) and the total average number of cleaved caspase-3–positive cells ($n = 3$, six images per sample) of different groups. Data are shown as mean ± SEM and were analyzed using ANOVA followed by Tukey's post hoc test. $^{*}P < 0.05$, $^{**}P < 0.01$, $^{***}P < 0.001$, $^{****}P < 0.0001$. Each point shown in the bar charts indicates an individual data point.

Investigative Ophthalmology & Visual Science

Downloaded from m.iovs.org on 05/04/2024

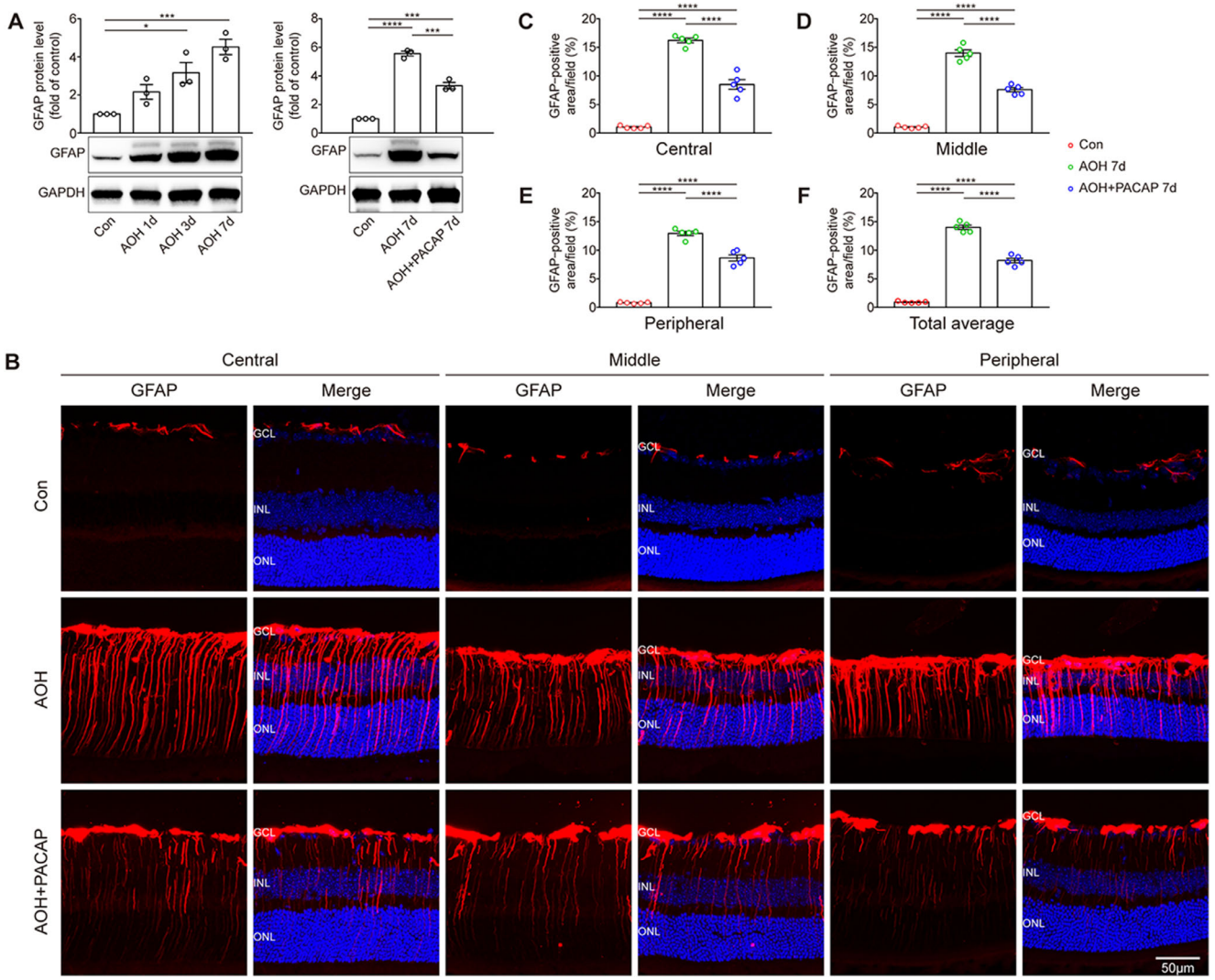

Figure 7. PACAP treatment inhibited the overactivation of macroglia including astrocytes and Müller cells induced by AOH injury. (**A**) The expression of GFAP was assessed by western blot. GAPDH was used to ensure equal loading ($n = 3$). (**B**) Representative images of retinal frozen sections labeled with GFAP (*red*) and DAPI (*blue*) 7 days after AOH injury (magnification 40×). (**C–F**) Bar charts showing the quantitative analyses of the percentage of GFAP-positive areas in the central, middle, and peripheral areas of the retina ($n = 5$, two images per sample) and the total average of these areas ($n = 5$, six images per sample). Data are shown as mean ± SEM and were analyzed using ANOVA followed by Tukey's post hoc test. $^{*}P < 0.05$, $^{***}P < 0.001$, $^{****}P < 0.0001$. Each point shown in the bar charts indicates an individual data point.

Discussion

The neuroprotective effects and underlying mechanisms of PACAP in mice models of AOH injury were not verified in previous studies. Our results found that PACAP treatment prevented the losses of retinal tissue and maintained the survival and function of RGCs after AOH injury. PACAP treatment could inhibit the apoptosis in AOH injury possibly through the modulation of apoptosis-related factors. In addition, PACAP treatment effectively suppressed reactive gliosis, retinal vascular inflammation, and activation of the NF-κB pathway in AOH injury.

Irreversible losses of retinal layers and impairment of visual function are common features in rodent models of AOH injury.[32] In the current study, H&E staining results showed that the thickness of the whole retina and sublayers of the inner retina (NFL/GCL, IPL, INL) was significantly reduced after AOH injury; these results are similar to those of previous studies.[17,32] This finding was further confirmed by non-invasive SD-OCT examination performed in live mice. Atlasz et al.[12] found that intravitreal injection of PACAP effectively prevented the loss of retina tissues induced by excitotoxic retinal injury. Similarly, our results demonstrate that PACAP could prevent the loss of retina tissue, especially that of the inner retina, in AOH injury. Furthermore, we also found that PACAP treatment markedly improved the survival of RGCs in AOH injury as observed in Tuj1 labeling. Corresponding to the significant decrease of RGC counts in AOH injury, the function of RGCs as assessed by PERG was found to be significantly damaged in AOH injury. The effect of PACAP on the function of RGCs in AOH injury has not been investigated before. We found that PERG amplitude was well preserved by PACAP treatment in AOH injury. Together with our previous study conducted in a rat model of ONC, which found that PACAP significantly improved the survival of RGCs in ONC injury,[15] PACAP has

Downloaded from m.iovs.org on 05/04/2024

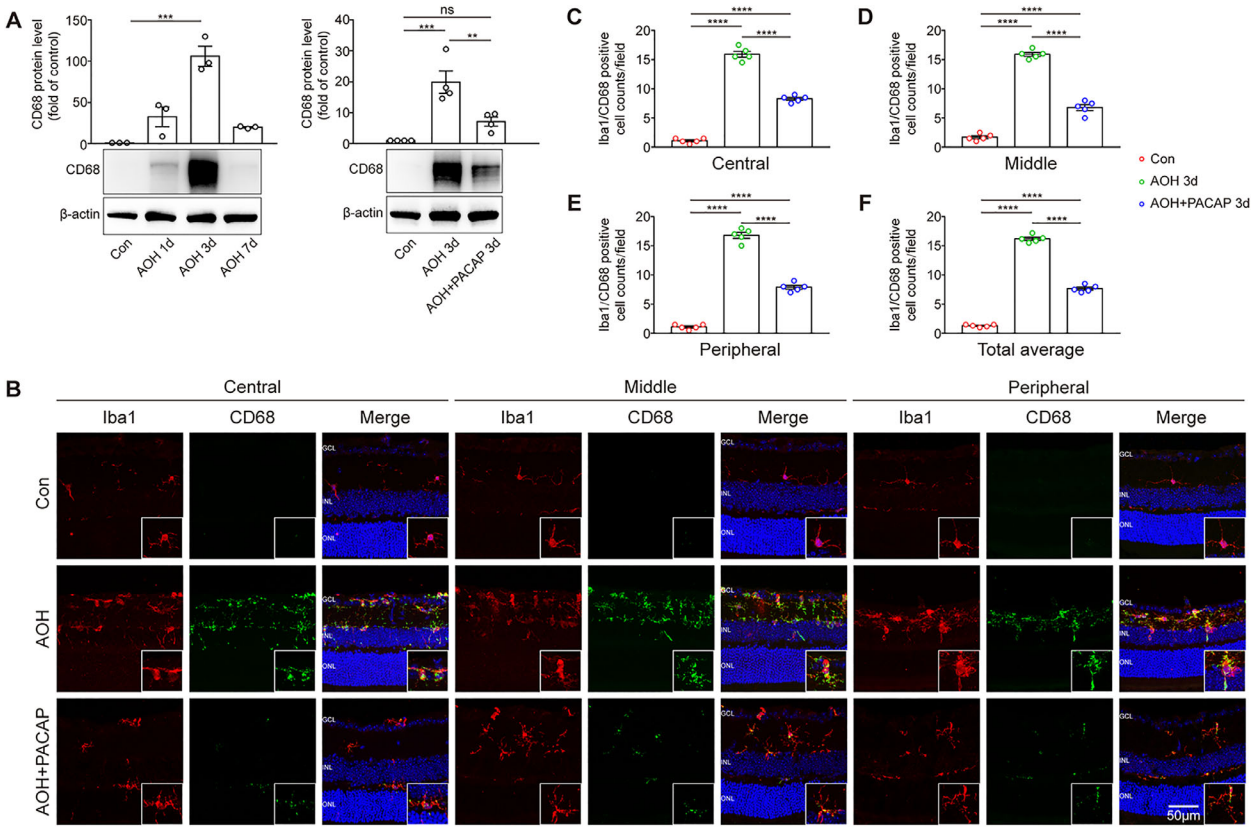

Figure 8. PACAP treatment inhibited the overactivation of microglial/macrophage cells. Overall microglial/macrophage cells were labeled by Iba1, and the activated microglial/macrophage cells were labeled by CD68. (**A**) The expression of CD68 was evaluated by western blot; β-actin was used to ensure equal loading ($n = 3$–5). (**B**) Representative images of retinal frozen sections double labeled by Iba1 (*red*), CD68 (*green*), and DAPI (*blue*) 3 days after AOH injury. Inset images are at higher magnifications of the representative microglia/macrophages. (**C–F**) Bar charts showing quantitative analyses of the average Iba1/CD68-positive cell counts in the central, middle, and peripheral areas of the retina ($n = 5$, two images per sample) and the total average number of Iba1/CD68-positive cells ($n = 5$, six images per sample) of different groups. Data are shown as mean ± SEM and were analyzed using ANOVA followed by Tukey's post hoc test. $^{**}P < 0.01$, $^{***}P < 0.001$, $^{****}P < 0.0001$. Each point shown in the bar charts indicates an individual data point.

demonstrated remarkable neuroprotective effects in relation to glaucoma.

Apoptosis, a programmed cell death pathway, has been hypothesized to be involved in the neurodegeneration of glaucoma.[33,34] In line with previous studies,[17,18] we found that TUNEL-positive cells were significantly increased in the GCL and INL after AOH injury, whereas the change was redressed when treated with PACAP. Notably, TUNEL positivity is not limited to apoptotic cells, as necrotic cells are TUNEL positive, as well.[35] Although TUNEL staining shows high sensitivity in distinguishing apoptosis from necrosis,[36] the results of TUNEL staining in the current study were not concrete evidence but a strong suggestion that PACAP exerts a potent anti-apoptotic effect in AOH injury.

To further understand whether and how PACAP was involved in apoptosis, we investigated several apoptosis-related factors, including Bim, Bax, Bcl-xL, and cleaved caspase-3. Bax is a proapoptotic factor that responds to apoptotic stimuli and promotes intrinsic apoptosis.[37,38] Bim belongs to the BH3-only protein family and was found to be a main direct activator of Bax.[38] Bcl-xL, a anti-apoptotic factor, inhibits the intrinsic apoptosis pathway by preventing the release of cytochrome *c* from mitochondria,[39] but caspase-3 is a principle executor of intrinsic and extrinsic apoptosis and is cleaved by various proteases to be activated (i.e., cleaved caspase-3).[40] The current study investigated time-course changes in these factors and found that Bim, Bax, and cleaved caspase-3 were significantly upregulated and peaked at day 3, whereas Bcl-xL was downregulated and was most significant 7 days after AOH injury. The results were similar to those of several previous studies.[41–43] However, these changes were reversed following PACAP treatment. The anti-apoptotic effect of PACAP is mainly mediated through the PAC1 receptor in central nervous system and retinal disorders,[44,45] and the PAC1 receptor was found to upregulate in ONC injury, as shown in our previous study.[46] The PAC1 receptor is associated with several pathways, including the adenylyl cyclase/protein kinase A pathway and the phosphatidylinositol 3′-OH kinase/Akt pathway, through which PACAP acts on intrinsic apoptosis-related factors and subsequently caspase-3 activity in central nervous system and retinal disorders.[44,45] Together, our results indicate that PACAP treatment exerts a potent anti-apoptotic effect in AOH injury that is, at least in part, associated with the modulation of apoptosis-related factors.

The normal retina works through interactions among neurons, glial cells, and blood vessels. Reactive gliosis has been reported to be associated with the neurodegeneration of glaucoma.[27,47] Macroglia, including astrocytes and Müller cells, are major glial cells in the retina, as these cells

Downloaded from m.iovs.org on 05/04/2024

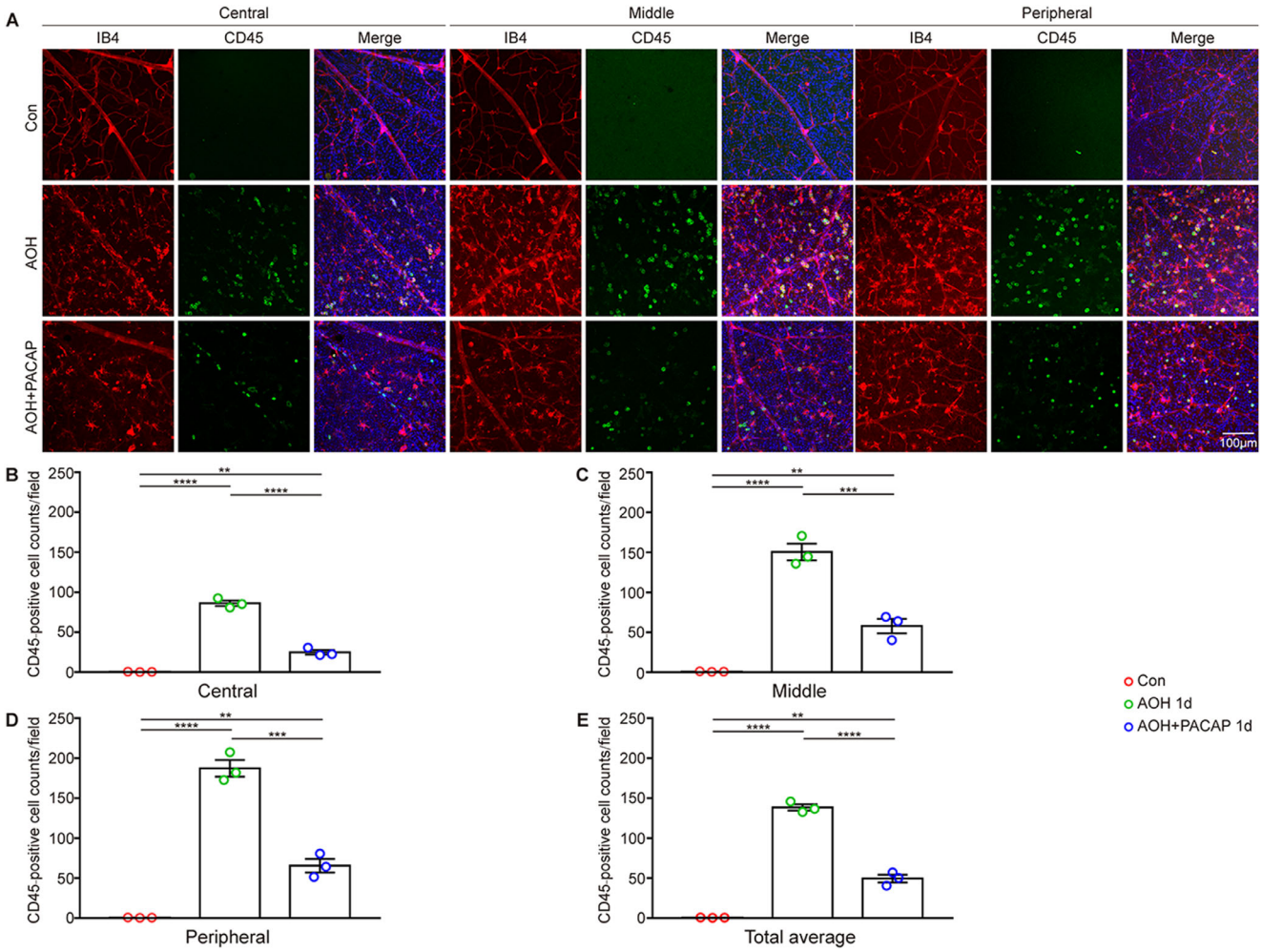

Figure 9. PACAP treatment alleviated the retinal vascular inflammation induced by AOH injury. Retinal blood vessels were labeled with IB_4, and leukocytes were labeled with CD45. (**A**) Representative images of retinal flatmounts labeled with CD45 (*green*), IB_4 (*red*), and DAPI (*blue*) 1 day after AOH injury. (**B–E**) Bar charts showing the quantitative analyses of CD45-positive leukocyte counts in the central, middle, and peripheral areas of the retina ($n = 3$, four images per sample) and the total average number of CD45-positive leukocytes ($n = 3$, 12 images per sample) of different groups. Data are shown as mean ± SEM and analyzed using ANOVA followed by Tukey's post hoc test. $^{**}P < 0.01$, $^{***}P < 0.001$, $^{****}P < 0.0001$. Each point shown in the bar charts indicates an individual data point.

supply nutrients to RGCs, support neuroretina structure, and mediate neuronal signal transmission.[48,49] AOH injury could induce reactive gliosis of macroglia, characterized by significant upregulation of GFAP and enhanced migration.[17,27] In line with these studies, the current study found that the expression of GFAP was markedly upregulated, processes of GFAP-positive cells were elongated extending from the NFL to ONL, and somas were thickened in the NFL and GCL after AOH injury. These changes were significantly attenuated by PACAP treatment. Microglial cells, which are located in the IPL and OPL in normal retina, are resident immune cells of the central nervous system and retina.[50] Injury triggers the rapid activation of microglial cells, which subsequently transition from a surveillance to a shielding state. However, pathological activation of microglial cells is hypothesized to aggravate neurodegenerative diseases, including glaucoma.[51,52] In the current study, we found that the number of reactive microglia/macrophages labeled with Iba1 and CD68 was significantly increased after AOH injury. In addition, activated microglia/macrophages were found to migrate from the IPL and OPL to the GCL and INL, and the morphology of the microglia/macrophages switched from a dendritic-shape to an ameboid-shape after AOH injury. These results were consistent with previous studies.[53,54] These changes were partly reversed by PACAP treatment, which is similar to the findings of a study by Kim et al.,[55] which reported that PACAP effectively inhibited the activation of microglia/macrophages induced by lipopolysaccharide. These results suggest that the neuroprotective effect of PACAP might partly be associated with the suppression of reactive gliosis in AOH injury.

Leukocyte attachment to retinal vessels and infiltration into the retina are hallmarks of vascular inflammation, which was found to occur soon after AOH injury and accelerated retinal neuronal injury.[18,56–58] Similarly, we found that the number of CD45-positive leukocytes was significantly increased after AOH injury. In addition, CD45-positive leukocytes were present mainly in intermediate-sized peripheral blood vessels and infiltrated into the retina after AOH injury. Riera et al.[59] found that PACAP could

Investigative Ophthalmology & Visual Science

Downloaded from m.iovs.org on 05/04/2024

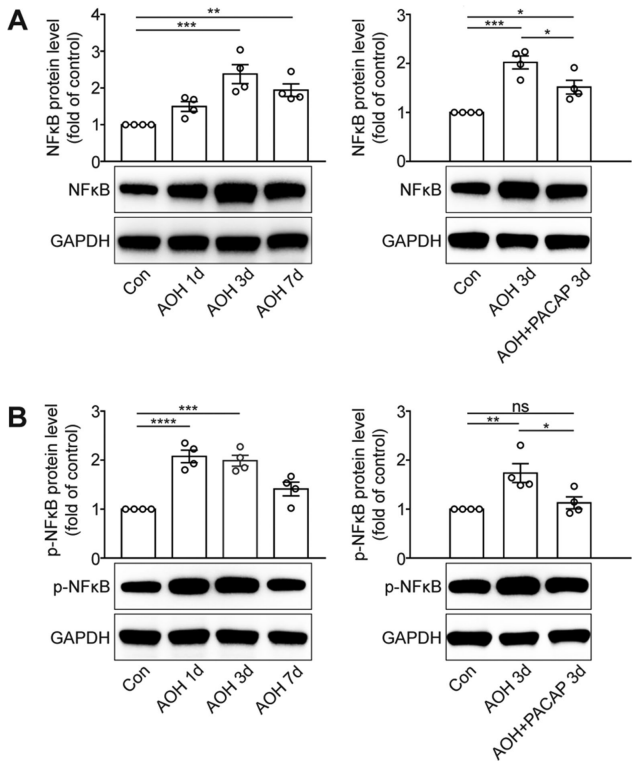

Figure 10. PACAP treatment inhibited the activation of the NF-κB pathway induced by AOH injury. (**A**) The expression of NF-κB was evaluated by western blot. GAPDH was used to ensure equal loading ($n = 4$). (**B**) The expression of p-NF-κB was evaluated by western blot. GAPDH was used to ensure equal loading ($n = 4$). Data are shown as mean ± SEM and were analyzed using ANOVA followed by Tukey's post hoc test. $^{*}P < 0.05$, $^{**}P < 0.01$, $^{***}P < 0.001$, $^{****}P < 0.0001$. Each point shown in the bar charts indicates an individual data point.

significantly reduce the number of CD45-positive leukocytes in renal ischemia/reperfusion injury. However, whether PACAP can reduce the number of CD45-positive leukocytes in AOH injury remain unknown. In the current study, we found that these changes were effectively redressed following treatment by PACAP. Collectively, our results indicate that PACAP treatment improves RGC survival at least partly by inhibiting retinal vascular inflammation in AOH injury.

An abundance of evidence has shown that the ubiquitously expressed transcriptional factor NF-κB plays an essential role in inflammatory processes, including reactive gliosis and vascular inflammation.[60–62] In response to injury, activated NF-κB undergoes nuclear translocation and binds to corresponding DNA sites, thereby promoting the transcription of proinflammatory factors.[63] A previous study found that PACAP treatment attenuated kidney ischemia/reperfusion injury by suppressing the NF-κB pathway.[64] However, the effect of PACAP on modulation of the NF-κB pathway in AOH injury remains unknown. In the current study, we found that both NF-κB and p-NF-κB expression levels were increased after AOH injury, whereas PACAP treatment significantly inhibited the upregulation of NF-κB and NF-κB phosphorylation. PACAP was found to act on the NF-κB pathway, most likely through the PAC1 receptor.[65,66] Our results suggest that the anti-inflammatory effect of PACAP might, at least in part, be associated with inhibition of the NF-κB pathway.

In summary, the current study provides convincing evidence that intravitreal injection of PACAP prevents the loss of retinal tissue and improves the survival and function of RGCs in AOH injury. These results can possibly be explained by the potent anti-apoptosis and anti-inflammation effects of PACAP. This study has identified PACAP as a promising therapeutic option for the treatment of glaucoma.

Acknowledgments

The authors thank Matthew Fan (Yale University, New Haven, CT) for proofreading our manuscript.

Supported by the Natural Science Foundation of Guangdong Province in China (2021A1515012142), Young Scientists Fund of the National Natural Science Foundation of China (81900864), and a research grant from Guangzhou Municipal Science and Technology Bureau in China (202102010324).

Disclosure: **P. Lu**, None; **Y. Shi**, None; **D. Ye**, None; **X. Lu**, None; **X. Tang**, None; **L. Cheng**, None; **Y. Xu**, None; **J. Huang**, None

References

1. Jonas JB, Aung T, Bourne RR, Bron AM, Ritch R, Panda-Jonas S. Glaucoma. *Lancet.* 2017;390(10108):2183–2193.
2. Chan PP, Pang JC, Tham CC. Acute primary angle closure-treatment strategies, evidences and economical considerations. *Eye*. 2019;33(1):110–119.
3. Sun X, Dai Y, Chen Y, et al. Primary angle closure glaucoma: what we know and what we don't know. *Prog Retin Eye Res*. 2017;57:26–45.
4. Pang IH, Clark AF. Inducible rodent models of glaucoma. *Prog Retin Eye Res*. 2020;75:100799.
5. Osborne NN, Casson RJ, Wood JP, Chidlow G, Graham M, Melena J. Retinal ischemia: mechanisms of damage and potential therapeutic strategies. *Prog Retin Eye Res*. 2004;23(1):91–147.
6. Miyata A, Arimura A, Dahl RR, et al. Isolation of a novel 38 residue-hypothalamic polypeptide which stimulates adenylate cyclase in pituitary cells. *Biochem Biophys Res Commun*. 1989;164(1):567–574.
7. Gábriel R, Pöstyéni E, Dénes V. Neuroprotective potential of pituitary adenylate cyclase activating polypeptide in retinal degenerations of metabolic origin. *Front Neurosci*. 2019;13:1031.
8. Shioda S, Nakamachi T. PACAP as a neuroprotective factor in ischemic neuronal injuries. *Peptides*. 2015;72:202–207.
9. Rat D, Schmitt U, Tippmann F, et al. Neuropeptide pituitary adenylate cyclase-activating polypeptide (PACAP) slows down Alzheimer's disease-like pathology in amyloid precursor protein-transgenic mice. *FASEB J*. 2011;25(9):3208–3218.
10. Reglodi D, Lubics A, Tamás A, Szalontay L, Lengvári I. Pituitary adenylate cyclase activating polypeptide protects dopaminergic neurons and improves behavioral deficits in a rat model of Parkinson's disease. *Behav Brain Res*. 2004;151(1-2):303–312.
11. Dejda A, Seaborn T, Bourgault S, et al. PACAP and a novel stable analog protect rat brain from ischemia: insight into the mechanisms of action. *Peptides*. 2011;32(6):1207–1216.
12. Atlasz T, Szabadfi K, Reglodi D, et al. Effects of pituitary adenylate cyclase activating polypeptide and its fragments on retinal degeneration induced by neonatal monosodium glutamate treatment. *Ann N Y Acad Sci*. 2009;1163:348–352.

Downloaded from m.iovs.org on 05/04/2024

13. Endo K, Nakamachi T, Seki T, et al. Neuroprotective effect of PACAP against NMDA-induced retinal damage in the mouse. *J Mol Neurosci*. 2011;43(1):22–29.
14. Wada Y, Nakamachi T, Endo K, et al. PACAP attenuates NMDA-induced retinal damage in association with modulation of the microglia/macrophage status into an acquired deactivation subtype. *J Mol Neurosci*. 2013;51(2):493–502.
15. Ye D, Shi Y, Xu Y, Huang J. PACAP attenuates optic nerve crush-induced retinal ganglion cell apoptosis via activation of the CREB-Bcl-2 pathway. *J Mol Neurosci*. 2019;68(3):475–484.
16. Seki T, Itoh H, Nakamachi T, et al. Suppression of rat retinal ganglion cell death by PACAP following transient ischemia induced by high intraocular pressure. *J Mol Neurosci*. 2011;43(1):30–34.
17. Luo H, Zhuang J, Hu P, et al. Resveratrol delays retinal ganglion cell loss and attenuates gliosis-related inflammation from ischemia-reperfusion injury. *Invest Ophthalmol Vis Sci*. 2018;59(10):3879–3888.
18. Liu W, Ha Y, Xia F, et al. Neuronal Epac1 mediates retinal neurodegeneration in mouse models of ocular hypertension. *J Exp Med*. 2020;217(4):e20190930.
19. Wan P, Su W, Zhang Y, et al. LncRNA H19 initiates microglial pyroptosis and neuronal death in retinal ischemia/reperfusion injury. *Cell Death Differ*. 2020;27(1):176–191.
20. Stankowska DL, Dibas A, Li L, et al. Hybrid Compound SA-2 is neuroprotective in animal models of retinal ganglion cell death. *Invest Ophthalmol Vis Sci*. 2019;60(8):3064–3073.
21. Berger S, Savitz SI, Nijhawan S, et al. Deleterious role of TNF-alpha in retinal ischemia-reperfusion injury. *Invest Ophthalmol Vis Sci*. 2008;49(8):3605–3610.
22. Abcouwer SF, Shanmugam S, Muthusamy A, et al. Inflammatory resolution and vascular barrier restoration after retinal ischemia reperfusion injury. *J Neuroinflammation*. 2021;18(1):186.
23. Huang R, Xu Y, Lu X, et al. Melatonin protects inner retinal neurons of newborn mice after hypoxia-ischemia. *J Pineal Res*. 2021;71(1):e12716.
24. Bach M, Brigell MG, Hawlina M, et al. ISCEV standard for clinical pattern electroretinography (PERG): 2012 update. *Doc Ophthalmol*. 2013;126(1):1–7.
25. Mohan K, Harper MM, Kecova H, et al. Characterization of structure and function of the mouse retina using pattern electroretinography, pupil light reflex, and optical coherence tomography. *Vet Ophthalmol*. 2012;15(suppl 2):94–104.
26. Lam TT, Abler AS, Tso MO. Apoptosis and caspases after ischemia-reperfusion injury in rat retina. *Invest Ophthalmol Vis Sci*. 1999;40(5):967–975.
27. Renner M, Stute G, Alzureiqi M, et al. Optic nerve degeneration after retinal ischemia/reperfusion in a rodent model. *Front Cell Neurosci*. 2017;11:254.
28. Perego C, Fumagalli S, De Simoni MG. Temporal pattern of expression and colocalization of microglia/macrophage phenotype markers following brain ischemic injury in mice. *J Neuroinflammation*. 2011;8:174.
29. Crespo-Castrillo A, Yanguas-Casás N, Arevalo MA, Azcoitia I, Barreto GE, Garcia-Segura LM. The synthetic steroid tibolone decreases reactive gliosis and neuronal death in the cerebral cortex of female mice after a stab wound injury. *Mol Neurobiol*. 2018;55(11):8651–8667.
30. Goebel U, Scheid S, Spassov S, et al. Argon reduces microglial activation and inflammatory cytokine expression in retinal ischemia/reperfusion injury. *Neural Regen Res*. 2021;16(1):192–198.
31. Zhang XY, Xiao YQ, Zhang Y, Ye W. Protective effect of pioglitazone on retinal ischemia/reperfusion injury in rats. *Invest Ophthalmol Vis Sci*. 2013;54(6):3912–3921.
32. Kim BJ, Braun TA, Wordinger RJ, Clark AF. Progressive morphological changes and impaired retinal function associated with temporal regulation of gene expression after retinal ischemia/reperfusion injury in mice. *Mol Neurodegener*. 2013;8:21.
33. Alqawlaq S, Flanagan JG, Sivak JM. All roads lead to glaucoma: induced retinal injury cascades contribute to a common neurodegenerative outcome. *Exp Eye Res*. 2019;183:88–97.
34. Moazzeni H, Khani M, Elahi E. Insights into the regulatory molecules involved in glaucoma pathogenesis. *Am J Med Genet C Semin Med Genet*. 2020;184(3):782–827.
35. Majtnerová P, Roušar T. An overview of apoptosis assays detecting DNA fragmentation. *Mol Biol Rep*. 2018;45(5):1469–1478.
36. Kelly KJ, Sandoval RM, Dunn KW, Molitoris BA, Dagher PC. A novel method to determine specificity and sensitivity of the TUNEL reaction in the quantitation of apoptosis. *Am J Physiol Cell Physiol*. 2003;284(5):C1309–1318.
37. Donahue RJ, Maes ME, Grosser JA, et al. BAX-depleted retinal ganglion cells survive and become quiescent following optic nerve damage. *Mol Neurobiol*. 2020;57(2):1070–1084.
38. Maes ME, Schlamp CL, Nickells RW. BAX to basics: how the BCL2 gene family controls the death of retinal ganglion cells. *Prog Retin Eye Res*. 2017;57:1–25.
39. Lopez J, Tait SWG. Mitochondrial apoptosis: killing cancer using the enemy within. *Br J Cancer*. 2015;112(6):957–962.
40. McIlwain DR, Berger T, Mak TW. Caspase functions in cell death and disease. *Cold Spring Harb Perspect Biol*. 2013;5(4):a008656.
41. Yang J, Yang N, Luo J, et al. Overexpression of S100A4 protects retinal ganglion cells against retinal ischemia-reperfusion injury in mice. *Exp Eye Res*. 2020;201:108281.
42. Abbasi M, Gupta VK, Chitranshi N, et al. Caveolin-1 ablation imparts partial protection against inner retinal injury in experimental glaucoma and reduces apoptotic activation. *Mol Neurobiol*. 2020;57(9):3759–3784.
43. Ju WK, Shim MS, Kim KY, et al. Ubiquinol promotes retinal ganglion cell survival and blocks the apoptotic pathway in ischemic retinal degeneration. *Biochem Biophys Res Commun*. 2018;503(4):2639–2645.
44. Dejda A, Jolivel V, Bourgault S, et al. Inhibitory effect of PACAP on caspase activity in neuronal apoptosis: a better understanding towards therapeutic applications in neurodegenerative diseases. *J Mol Neurosci*. 2008;36(1-3):26–37.
45. Seaborn T, Masmoudi-Kouli O, Fournier A, Vaudry H, Vaudry D. Protective effects of pituitary adenylate cyclase-activating polypeptide (PACAP) against apoptosis. *Curr Pharm Des*. 2011;17(3):204–214.
46. Ye D, Yang Y, Lu X, et al. Spatiotemporal expression changes of PACAP and its receptors in retinal ganglion cells after optic nerve crush. *J Mol Neurosci*. 2019;68(3):465–474.
47. Palmhof M, Wagner N, Nagel C, et al. Retinal ischemia triggers early microglia activation in the optic nerve followed by neurofilament degeneration. *Exp Eye Res*. 2020;198:108133.
48. de Hoz R, Rojas B, Ramírez AI, et al. Retinal macroglial responses in health and disease. *Biomed Res Int*. 2016;2016:2954721.
49. Sorrentino FS, Allkabes M, Salsini G, Bonifazzi C, Perri P. The importance of glial cells in the homeostasis of the retinal microenvironment and their pivotal role in the course of diabetic retinopathy. *Life Sci*. 2016;162:54–59.
50. Rashid K, Akhtar-Schaefer I, Langmann T. Microglia in retinal degeneration. *Front Immunol*. 2019;10:1975.

Investigative Ophthalmology & Visual Science

Downloaded from m.iovs.org on 05/04/2024

51. Perry VH, Holmes C. Microglial priming in neurodegenerative disease. *Nat Rev Neurol*. 2014;10(4):217–224.
52. Ramírez AI, Salazar JJ, de Hoz R, et al. Macro- and microglial responses in the fellow eyes contralateral to glaucomatous eyes. *Prog Brain Res*. 2015;220:155–172.
53. Hu T, Wang S, Zeng L, Xiong K, Chen D, Huang J. Regional expression of Act-MMP3 contributes to the selective loss of neurons in ganglion cell layers following acute retinal ischemia/reperfusion injury. *Curr Eye Res*. 2020;45(5):591–603.
54. Silverman SM, Kim BJ, Howell GR, et al. C1q propagates microglial activation and neurodegeneration in the visual axis following retinal ischemia/reperfusion injury. *Mol Neurodegener*. 2016;11:24.
55. Kim WK, Ganea D, Jonakait GM. Inhibition of microglial CD40 expression by pituitary adenylate cyclase-activating polypeptide is mediated by interleukin-10. *J Neuroimmunol*. 2002;126(1-2):16–24.
56. Gonçalves A, Lin CM, Muthusamy A, et al. Protective effect of a GLP-1 analog on ischemia-reperfusion induced blood-retinal barrier breakdown and inflammation. *Invest Ophthalmol Vis Sci*. 2016;57(6):2584–2592.
57. Abcouwer SF, Lin CM, Shanmugam S, Muthusamy A, Barber AJ, Antonetti DA. Minocycline prevents retinal inflammation and vascular permeability following ischemia-reperfusion injury. *J Neuroinflammation*. 2013;10:149.
58. Ha Y, Liu H, Xu Z, et al. Endoplasmic reticulum stress-regulated CXCR3 pathway mediates inflammation and neuronal injury in acute glaucoma. *Cell Death Dis*. 2015;6(10):e1900.
59. Riera M, Torras J, Cruzado JM, et al. The enhancement of endogenous cAMP with pituitary adenylate cyclase-activating polypeptide protects rat kidney against ischemia through the modulation of inflammatory response. *Transplantation*. 2001;72(7):1217–1223.
60. Saggu R, Schumacher T, Gerich F, et al. Astroglial NF-κB contributes to white matter damage and cognitive impairment in a mouse model of vascular dementia. *Acta Neuropathol Commun*. 2016;4(1):76.
61. Namyen J, Permpoonputtana K, Nopparat C, Tocharus J, Tocharus C, Govitrapong P. Protective effects of melatonin on methamphetamine-induced blood-brain barrier dysfunction in rat model. *Neurotox Res*. 2020;37(3):640–660.
62. Li J, Chen Y, Zhang X, et al. Inhibition of acetylcholinesterase attenuated retinal inflammation via suppressing NF-κB activation. *Exp Eye Res*. 2020;195:108003.
63. Gadjeva M, Tomczak MF, Zhang M, et al. A role for NF-kappa B subunits p50 and p65 in the inhibition of lipopolysaccharide-induced shock. *J Immunol*. 2004;173(9):5786–5793.
64. Khan AM, Li M, Abdulnour-Nakhoul S, Maderdrut JL, Simon EE, Batuman V. Delayed administration of pituitary adenylate cyclase-activating polypeptide 38 ameliorates renal ischemia/reperfusion injury in mice by modulating Toll-like receptors. *Peptides*. 2012;38(2):395–403.
65. Delgado M, Munoz-Elias EJ, Gomariz RP, Ganea D. Vasoactive intestinal peptide and pituitary adenylate cyclase-activating polypeptide prevent inducible nitric oxide synthase transcription in macrophages by inhibiting NF-kappa B and IFN regulatory factor 1 activation. *J Immunol*. 1999;162(8):4685–4696.
66. Delgado M. Vasoactive intestinal peptide and pituitary adenylate cyclase-activating polypeptide inhibit CBP-NF-kappaB interaction in activated microglia. Delgado M. Vasoactive intestinal peptide and pituitary adenylate cyclase-activating polypeptide inhibit CBP-NF-kappaB interaction in activated microglia. *Biochem Biophys Res Commun*. 2002;297(5):1181–1185.

Investigative Ophthalmology & Visual Science

Downloaded from m.iovs.org on 05/04/2024